Acta Crystallographica Section B
Structural Science
ISSN 0108-7681

Structures of $CsEuBr_3$ and its degradation product $Cs_2EuBr_5{\cdot}10H_2O$

Helmut Ehrenberg,[a]* Hartmut Fuess,[a] Sabine Hesse,[b] Jörg Zimmermann,[b] Heinz von Seggern[b] and Michael Knapp[a,c]

[a]Darmstadt University of Technology, Institute for Materials Science, Structural Research, Petersenstrasse 23, D-64287 Darmstadt, Germany, [b]Darmstadt University of Technology, Institute for Materials Science, Electronic Materials, Petersenstrasse 23, D-64287 Darmstadt, Germany, and [c]CELLS-ALBA, Apartado de correos 68, E-08193 Bellaterra, Spain

Correspondence e-mail: ehrenberg@tu-darmstadt.de

Received 17 May 2006
Accepted 16 November 2006

$CsEuBr_3$, caesium europium tribromide, crystallizes in an orthorhombic perovskite-type structure with an $a^-a^-c^+$ octahedral tilting scheme ($GdFeO_3$ type). $CsEuBr_3$ is unstable in air and one of the degradation products was identified as $Cs_2EuBr_5{\cdot}10H_2O$ by single-crystal X-ray analysis and synchrotron powder diffraction. The Eu^{3+} ions on twofold rotational axes are coordinated by nine water molecules, and each water O atom is linked to two Br atoms by hydrogen bonds. The tricapped trigonal $[EuO_9]$ prisms are separated from each other by infinite $\{Cs_2Br_5{\cdot}H_2O\}$ chains; the description $Eu(OH_2)_9Cs_2Br_5(OH_2)$ might therefore be more appropriate. The oxidation of Eu^{2+} to Eu^{3+} during the degradation of $CsEuBr_3$ is further confirmed by changes in the magnetic properties from the as-prepared material into the degraded product.

1. Introduction

Eu^{2+}-doped CsBr is a promising material as a photostimulable X-ray storage phosphor for high-resolution image plates (von Seggern, 1999; Schmitt *et al.*, 2002). The chemical environment of the Eu^{2+} ions is, however, not known and a segregation of $CsEuBr_3$ or Cs_4EuBr_6 was proposed (Hackenschmied *et al.*, 2003). The lack of structural data for $CsEuBr_3$ initiated this study and single crystals were prepared for X-ray structure determination. During an investigation of the photostimulated luminescence a degradation of $CsEuBr_3$ in air was observed (Hesse *et al.*, 2006). The X-ray powder diffraction pattern of the degraded material agrees well with the additional reflections observed by Hackenschmied *et al.* (2003) in $CsBr:Eu^{2+}$, besides those from CsBr. Therefore, the degradation products of $CsEuBr_3$ in air were also structurally characterized to elucidate the role of $CsEuBr_3$ in the photostimulation process of $CsBr:Eu^{2+}$.

2. Experimental

$CsEuBr_3$ was prepared by the route described by Nocera *et al.* (1980) for $CsEuCl_3$: CsBr (ultra dry quality, Alfa) and $EuBr_2$ (99.99%, Alfa, dried by heating under inert atmosphere at 473 K) were mixed in a 1:1 ratio by grinding in an agate mortar under a dry Ar atmosphere. The mixture was placed in silica tubes, which were sealed after evacuation to a pressure below 2×10^{-4} Pa. The tubes were tempered at 1123 K for 1 h before cooling to room temperature and then the tubes were opened under a dry Ar atmosphere in a glovebox. A single crystal of suitable quality for X-ray diffraction was selected under a light microscope, mounted on a glass fibre and protected against humidity by coating with an anhydrous glue. A separate

Table 1
Experimental details.

	(1)	(2)
Crystal data		
Chemical formula	Br_3CsEu	$Br_5Cs_2EuH_{20}O_{10}$
M_r	524.60	997.49
Cell setting, space group	Orthorhombic, *Pbnm*	Orthorhombic, *Pbcm*
Temperature (K)	299 (2)	299 (2)
a, b, c (Å)	8.242 (2), 8.3027 (18), 11.785 (2)	8.047 (2), 13.998 (3), 19.558 (2)
V (Å^3)	806.5 (3)	2203.1 (8)
Z	4	4
D_x (Mg m^{-3})	4.321	3.007
Radiation type	Mo $K\alpha$	Mo $K\alpha$
μ (mm^{-1})	26.97	15.20
Crystal form, colour	Prism, colourless transparent	Prism, colourless transparent
Crystal size (mm)	0.050 × 0.040 × 0.025	0.065 × 0.050 × 0.050
Data collection		
Diffractometer	Oxford Diffraction Xcalibur (TM) single-crystal X-ray diffractometer with sapphire CCD detector	Oxford Diffraction Xcalibur (TM) single-crystal X-ray diffractometer with sapphire CCD detector
Data collection method	Rotation method data acquisition using φ scans	Rotation method data acquisition using φ and ω scans
Absorption correction	Multi-scan	Multi-scan
T_{min}	0.244	0.456
T_{max}	0.532	0.610
No. of measured, independent and observed reflections	2878, 1051, 421	9144, 2488, 1231
Criterion for observed reflections	$I>4\sigma(I)$	$I>4\sigma(I)$
R_{int}	0.091	0.075
θ_{max} (°)	29.87	27.66
Refinement		
Refinement on	F^2	F^2
$R[F^2>2\sigma(F^2)]$, $wR(F^2)$, S	0.039, 0.079, 0.825	0.054, 0.0795, 0.928
No. of reflections	1051	2488
No. of parameters	28	89
Weighting scheme	$w = 1/[\sigma^2(F_o^2) + (0.0363P)^2]$, where $P = (F_o^2 + 2F_c^2)/3$	$w = 1/[\sigma^2(F_o^2) + (0.0422P)^2]$, where $P = (F_o^2 + 2F_c^2)/3$
$\Delta\rho_{max}$, $\Delta\rho_{min}$ (e Å^{-3})	2.08, −1.57	1.42, −1.07

amount of compound was ground under a dry Ar atmosphere and placed in a cuvette, which was sealed by parafilm for further investigations. Repeated determination of the photoluminescence properties of the same material, but after storing the previously studied cuvette in a desiccator for 12 months, revealed a partial degradation of the as-prepared material. The upper part of the material, closer to harmful moisture, showed a pink colour which is characteristic of Eu^{3+} formation, while the lower part remained blue under UV excitation (Hesse *et al.*, 2006). A single crystal from this degraded material could be selected out of the upper part of the cuvette and was also subjected to X-ray structure analysis. Details of the experimental conditions are summarized in Table 1. Powder diffraction experiments have been performed on the degraded material to reveal more information on the resulting product. Preliminary laboratory experiments gave rather complicated patterns, so that an additional data set was collected with better resolution at beamline B2 (Knapp *et al.*, 2004) of the Hamburger Synchrotronstrahlungslabor HASYLAB, Germany. The temperature dependence of the magnetization was measured for the as-prepared and degraded material in an applied field of 100 G using a superconducting interference device (SQUID) MPMS from Quantum Design.

3. Results and discussion

The as-prepared $CsEuBr_3$ compound crystallizes in a perovskite-type structure with an $a^-a^-c^+$ octahedral tilting scheme (Glazer, 1972), see Fig. 1, and is isotypic to $GdFeO_3$. The atomic parameters have been deposited in the CIF file.[1] Rietveld refinement of this $CsEuBr_3$ structure model confirmed the purity of the as-prepared material (Hesse *et al.*, 2006).

Structure solution based on single-crystal X-ray diffraction on the crystal from the degraded material revealed the composition $Cs_2EuBr_5{\cdot}10H_2O$ (see supplementary material for atomic parameters); Fig. 2 shows a graphical representation of this structure. This stoichiometry is in agreement with oxidation from Eu^{2+} to Eu^{3+}, as expected from the photoluminescence behaviour. The Eu^{3+} ions are surrounded by nine water molecules in such a way that tricapped trigonal $[EuO_9]$ prisms result, see Fig. 3. The H atoms cannot be located directly in this X-ray study, but the Br—O—Br angles suggest that they point from the O atoms to the nearest Br ions and thereby determine the orientations of the water molecules. A very similar coordination of a trivalent rare-earth element with water is observed in $HoBr_3{\cdot}8H_2O$, as shown in Fig. 4 (Junk *et al.*, 1999). In this paper the authors also discuss the number of water molecules and the structural systematics in $Ln^{III}Br_3{\cdot}nH_2O$ compounds. The proposed eightfold coordination for Ln = Ho, Lu and Y represents the 'maximally' hydrated rare-earth(III) bromides in this series. A sixfold coordination would be expected for Ln = Eu, as for Pr, Nd and Dy, but in contrast to the compounds of the latter elements the Eu compound was not studied. A similar ninefold coordination to that in $Cs_2EuBr_5{\cdot}10H_2O$ is reported for $Tb(H_2O)_9(BrO_3)_3$ (Gallucci *et al.*, 1982) and for the similar compound $Ho(BrO_3)_3{\cdot}9H_2O$ (Gerkin & Reppart, 1987). In the title compound infinite chains with the formal composition

[1] Supplementary data for this paper are available from the IUCr electronic archives (Reference: WS5050). Services for accessing these data are described at the back of the journal.

$\{Cs_2Br_5{\cdot}H_2O\}^{3-}$ exist (Fig. 5), so the stoichiometry is better written as $Eu(OH_2)_9Cs_2Br_5(OH_2)$.

$Eu(OH_2)_9Cs_2Br_5(OH_2)$ is indeed the main component in the degradation product of $CsEuBr_3$ in air, as confirmed by powder diffraction, see Fig. 6. At present it is not clear what additonal phase(s) is produced during degradation.

The temperature dependence of the magnetic susceptibility for as-prepared $CsEuBr_3$ obeys a modified Curie–Weiss law,

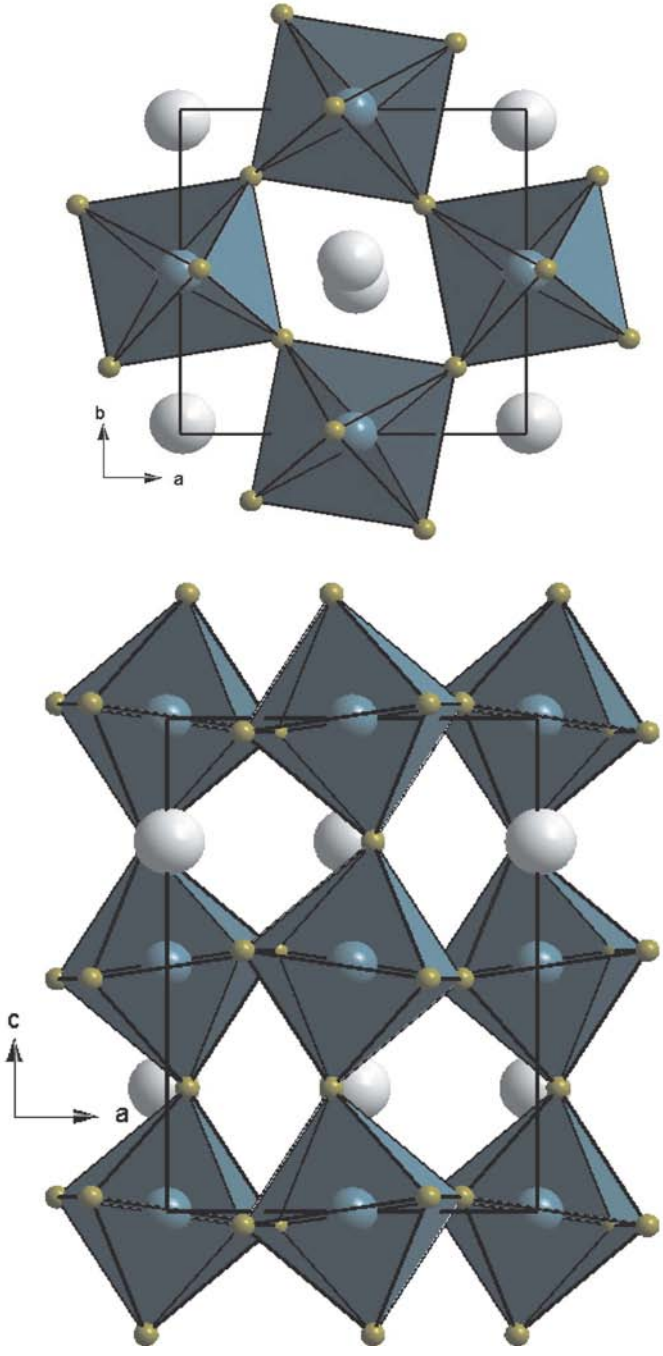

Figure 1
[$EuBr_6$] octahedral tiltings in $CsEuBr_3$.

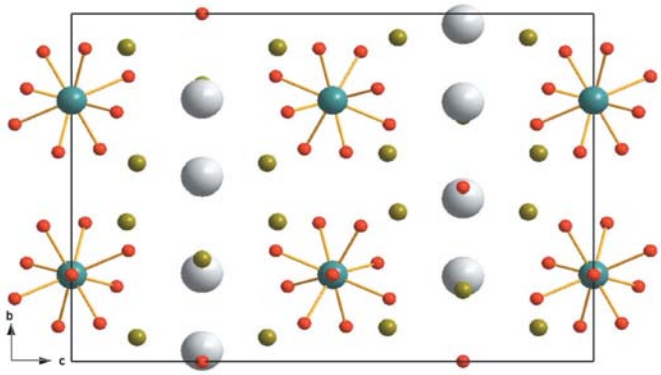

Figure 2
Crystal structure of $Cs_2EuBr_5{\cdot}10H_2O$. Br ions are shown olive-coloured, Cs ions in grey and Eu ions in blue. This figure is in colour in the electronic version of this paper.

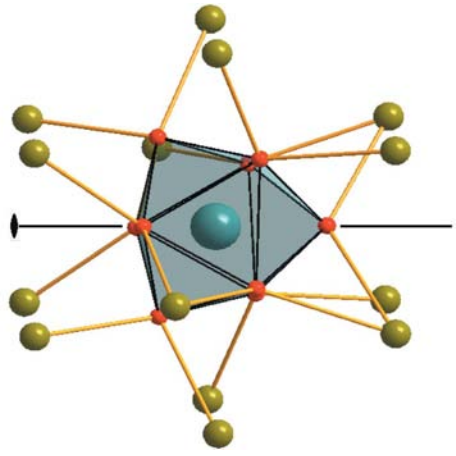

Figure 3
Coordination polyhedron of the Eu^{3+} ions in $Cs_2EuBr_5{\cdot}10H_2O$. The twofold rotational axis is also shown.

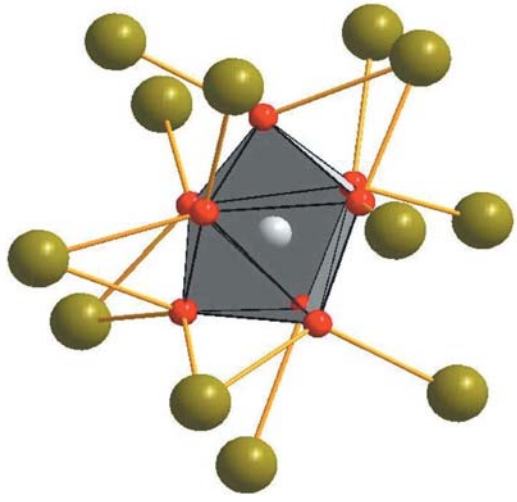

Figure 4
Coordination polyhedron of the Ho^{3+} ions in $HoBr_3{\cdot}8H_2O$ (Junk *et al.*, 1999). The eight O atoms form a bicapped trigonal [HoO_8] prism.

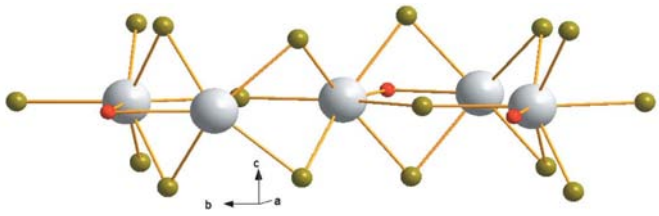

Figure 5
Chains along the *b* axis with the composition $\{Cs_2Br_5{\cdot}H_2O\}$.

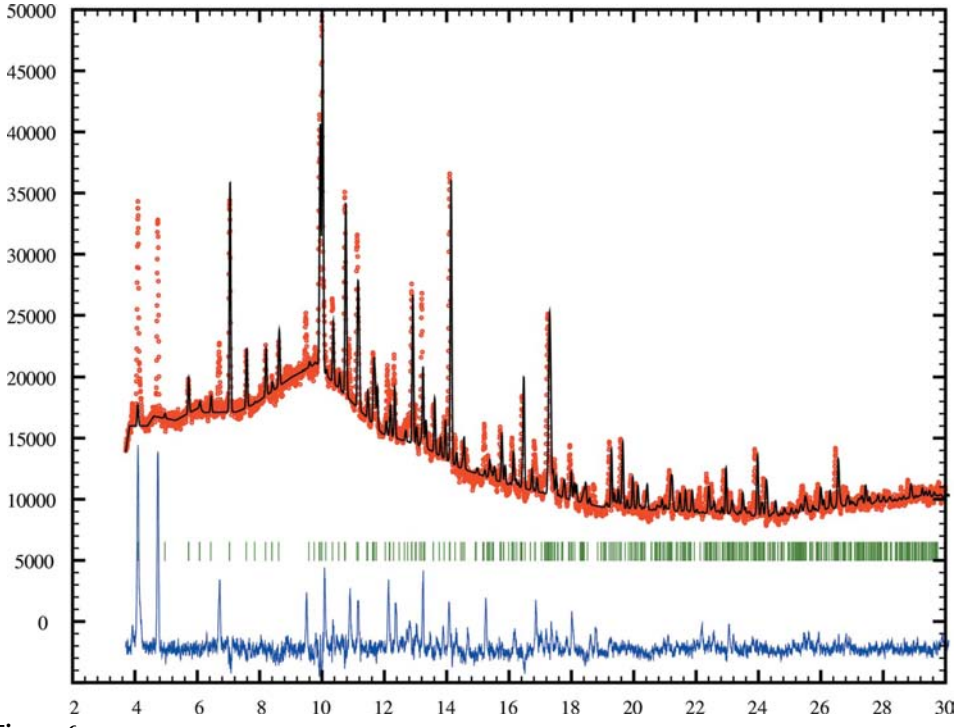

Figure 6
Synchrotron diffraction pattern [λ = 0.69838 (1) Å] for the degraded material. The solid drawn line is calculated based on the structure parameters of $Cs_2EuBr_5{\cdot}10H_2O$. The difference curve can be considered as a fingerprint of at least one more as yet unidentified phase in the sample.

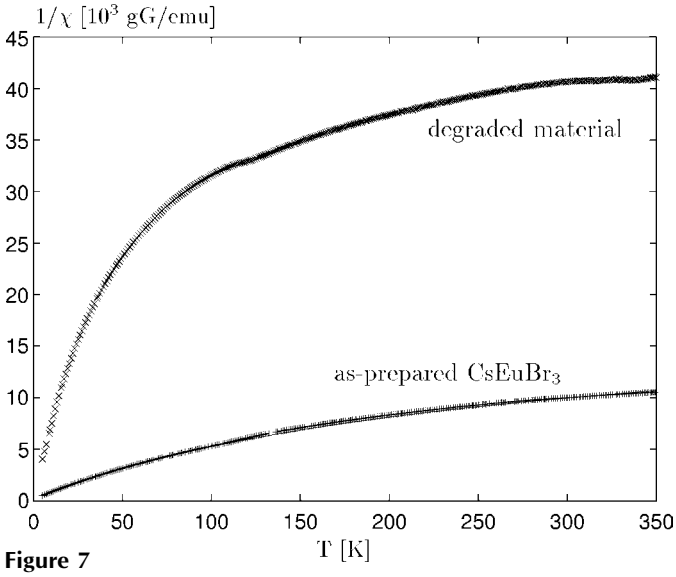

Figure 7
Inverse specific magnetic susceptibilities. Note that the drawn line for the modified Curie–Weiss fit to the $CsEuBr_3$ data can hardly be seen because of the high number of data points and the good agreement.

$\chi(T) = \frac{C}{T-\Theta} + \chi_0$, in the temperature range 5–350 K, with $\Theta = -2.4$ K, $\chi_0 = 53.4{\cdot}10^{-6}$ emu gG^{-1}, and a paramagnetic moment of $7.67\mu_B$ per Eu^{2+} ion (Fig. 7). A theoretical value of $7.94\mu_B$ is expected for an ideal $^8S_{7/2}$ state of the $4f^7$ electron configuration. The slightly lower experimental value might be the first indication of the onsetting degradation, accompanied by an oxidation from Eu^{2+} to Eu^{3+}. The highly degraded material shows a significantly reduced specific magnetic susceptibility (Fig. 7). Numerical values for the Eu moments for comparison cannot be derived, because the composition of the degraded material is not fully known.

4. Concluding remarks

The crystal structure of $CsEuBr_3$ has been determined as an orthorhombic perovskite-type modification, which is unstable in air. The improved photostimulated luminescence (PSL) of $CsBr:Eu^{2+}$ after annealing in air is not explained by the main degradation product of $CsEuBr_3$, which is $Eu(OH_2)_9Cs_2Br_5(OH_2)$ with Eu in the trivalent state. Additional phases were detected in the processing, but have not yet been identified. Investigations parallel to the PSL evolution, phase transformations and crystal structures including intermediate states seem mandatory in order to fully elucidate the relation between the PSL enhancement and the various crystalline phases.

References

Gallucci, J. C., Gerkin, R. E. & Reppart, W. J. (1982). *Cryst. Struct. Commun.* **11**, 1141–1145.
Gerkin, R. E. & Reppart, W. J. (1987). *Acta Cryst.* C**43**, 623–631.
Glazer, A. M. (1972). *Acta Cryst.* B**28**, 3384–3392.
Hackenschmied, P., Schierning, G., Batentschuk, M. & Winnacker, A. (2003). *J. Appl. Phys.* **93**, 5109–5112.
Hesse, S., Zimmermann, J., von Seggern, H., Ehrenberg, H., Fuess, H., Fasel, C. & Riedel, R. (2006). *J. Appl. Phys.* **100**, 083506.
Junk, P. C., Semenova, L. I., Skelton, B. W. & White, A. H. (1999). *Aust. J. Chem.* **52**, 531–538.
Knapp, M., Baehtz, C., Ehrenberg, H. & Fuess, H. (2004). *J. Synchrotron Rad.* **11**, 328–334.
Nocera, D. G., Morss, L. R. & Fahey, J. A. (1980). *J. Inorg. Nucl. Chem.* **42**, 55–59.
Schmitt, B., Fuchs, M., Hell, E., Knüpfer, W., Hackenschmied, P. & Winnacker, A. (2002). *Nucl. Instrum. Methods B*, **191**, 800.
Seggern, H. von (1999). *Brazilian J. Phys.* **29**, 254.